Materials Advances

ROYAL SOCIETY OF CHEMISTRY

COMMUNICATION

View Article Online
View Journal | View Issue

Cite this: *Mater. Adv.*, 2021, 2, 5906

Received 5th July 2021,
Accepted 18th August 2021

DOI: 10.1039/d1ma00575h

rsc.li/materials-advances

Simple/efficient solution-processed emitting systems dominated by a novel bipolar small-molecule iridium(III) complex†

Yu Feng,[a] Jianan Xue,[a] Hao Zhang,*[b] Tong Lu,[a] Kaiqi Ye,[a] Yu Liu*[a] and Yue Wang[a]

By incorporating two alkyl chains as the solubilizing groups, a new small-molecule bipolar phosphorescent complex FMPPHC dominates the highly efficient sky blue and saturated red wet-process emitting systems for organic light-emitting diodes (OLEDs).

Phosphorescent organic light-emitting diodes (PHOLEDs) with 100% utilization of the excitons are always the focus of attention for both academic groups and commercial companies, and have been widely used in flat panel displays and also have great potential in energy saving solid-state lighting.[1–4] So far almost all the highly efficient PHOLEDs are fabricated through a vacuum deposition process, which will lead to a high cost of the large-size products. Alternatively, solution processing technologies including spin coating and ink printing are more promising due to their simple and low-cost fabrication process for large size panel production.[5–7] As catalogued in the literature, the emitting systems of most current solution-processed PHOLEDs mainly adopt the following two strategies:[8–12] (i) phosphors doped in single/mixed fluorescent host materials possessing relatively high triplet energy, sufficient hole/electron transporting property and good solubility in common organic solvents. Their easy preparation/purification methods together with the corresponding structural optimization ensure the availability in sensitizing the dopant phosphors, but the precise control over the concentration of phosphorescent dopants and a certain degree of phase segregation in the corresponding doping systems are inevitable; (ii) phosphorescent Ir(III) complexes with oligomeric or polymeric ligand systems or dendrimers with high film densities and uniform film morphologies usually possess inherent advantages such as a simple fabrication process of the devices as well as good device stability and reproducibility. However, the deep-rooted inadequacies such as their uncertain molecular structures, additional multistep reaction sequences and the requirement for harsh purification always limit the incorporation of these materials in OLEDs.

Most recently, several PHOLEDs based on new-type doping emitting layers (EMLs) where both the host and guest are bipolar phosphorescent molecules, namely phosphor-only (PO) systems, achieve higher and more stable electroluminescence (EL) performance in monochromatic and white EL devices than the conventional fluorescent/phosphorescent doping cases.[13–15] It's well understood that all of the components in such PO doping combinations are phosphorescent iridium(III) complexes, so they possess more similar optoelectronic characteristics and better compatibility of molecular configuration than those hybrid cases. Therefore these PO emitting systems can effectively reduce the excited energy loss and ensure their excellent electro-phosphorescence properties: low driving voltages, high efficiencies with low efficiency roll-off, and even the remarkable doping concentration independent feature to a certain range. However, all these present bipolar phosphors are basically designed according to the requirement of thermal-deposition fabrication, and thus they usually easily crystallize based on the spin coating process and their film morphology is not stable enough, indicating that they are inappropriate for a wet-process method. In this work, a suitable-length alkyl chain (*n*-hexane) has been introduced into a small molecule-based phosphorescent complex to improve its film-forming ability and morphological stability based on solution processes, and meanwhile, this solubilizing group does not reduce the inherent good photoelectric characteristics of this bipolar phosphorescent material system. Thus we achieve a new sky-blue phosphorescent complex (**FMPPHC**) with good solubility toward organic solvents by employing 2′,6′-difluoro-4-methyl-2,3′-bipyridine (dfMepypy) as the

[a] *State Key Laboratory of Supramolecular Structure and Materials, Jilin University, Changchun 130012, P. R. China. E-mail: yuliu@jlu.edu.cn*
[b] *Zhejiang Brilliant Optoelectronic Technology Co., Ltd, No. 148 Yongda Road, Taizhou City 318020, P. R. China. E-mail: zhanghao_zj@qq.com*

† Electronic supplementary information (ESI) available: General information and experimental details including synthesis, single crystal, transient PL spectra of the new complex and device fabrication. CCDC 2073344. For ESI and crystallographic data in CIF or other electronic format see DOI: 10.1039/d1ma00575h

cyclometalated (C^N) ligand and 3,6-dihexyl-*N*,*N*′-diisopropyl-9*H*-carbazole-9-carboximidamide (Hxdipcca) as the ancillary ligand. As we expected, **FMPPHC** dominates the excellent EL performance originated from a series of spin-coating thin films: (i) a neat **FMPPHC** film-based emitting layer (EML) realizes efficient sky-blue EL with very high external quantum efficiency (EQE) and power efficiency (PE) of 16.5% and 32.3 lm W^{-1} respectively; (ii) a doped EML based on a red dopant phosphor BTPBA dispersed in the **FMPPHC** host adopting quite high and large-span doping concentrations of 15 and 30 wt% achieves EQE and PE values of more than 20% and 25 lm W^{-1} respectively and exhibits stable saturated red emission (λ_{max} = 616 nm) with the Commission Internationale de L'Eclairage ($CIE_{x,y}$) coordinates of (0.64, 0.36). Although such EL performance is not the highest efficiency level for the current wet-process OLEDs,[16–23] it is worth mentioning that, this indeed is the first achievement of the PHOLED employing the advanced PO emitting systems *via* the solution-processing method, and thus represents a promising way to develop wet-process feasible small-molecule phosphorescent complexes being used as new-concept emitting/host materials for generating/sensitizing more efficient EL in OLEDs.

As a new phosphorescent complex, the high-yield synthesis of **FMPPHC** is depicted in Scheme S1 of the ESI.†[24–26] The NMR, MS and mass element analysis spectral investigations confirm the molecular structure of this Ir(III) complex, and its molecular structure in single crystals is determined by X-ray diffraction. As shown in Fig. 1a, two long *n*-hexane chains have been introduced into the ancillary ligand of **FMPPHC**, which can effectively reduce the intermolecular interaction between the adjacent complex molecules and then bread the stacking structure in their solid state. This should be the major factor necessary to improve the solubility and film-forming ability of the metal complexes, and ensures the high performance of solution-processed OLEDs. From the ORTEP plot, **FMPPHC** exhibits distinct C,C-*cis* accompanied by N,N-*trans* configuration, where two cyclometalated ligands form a distorted

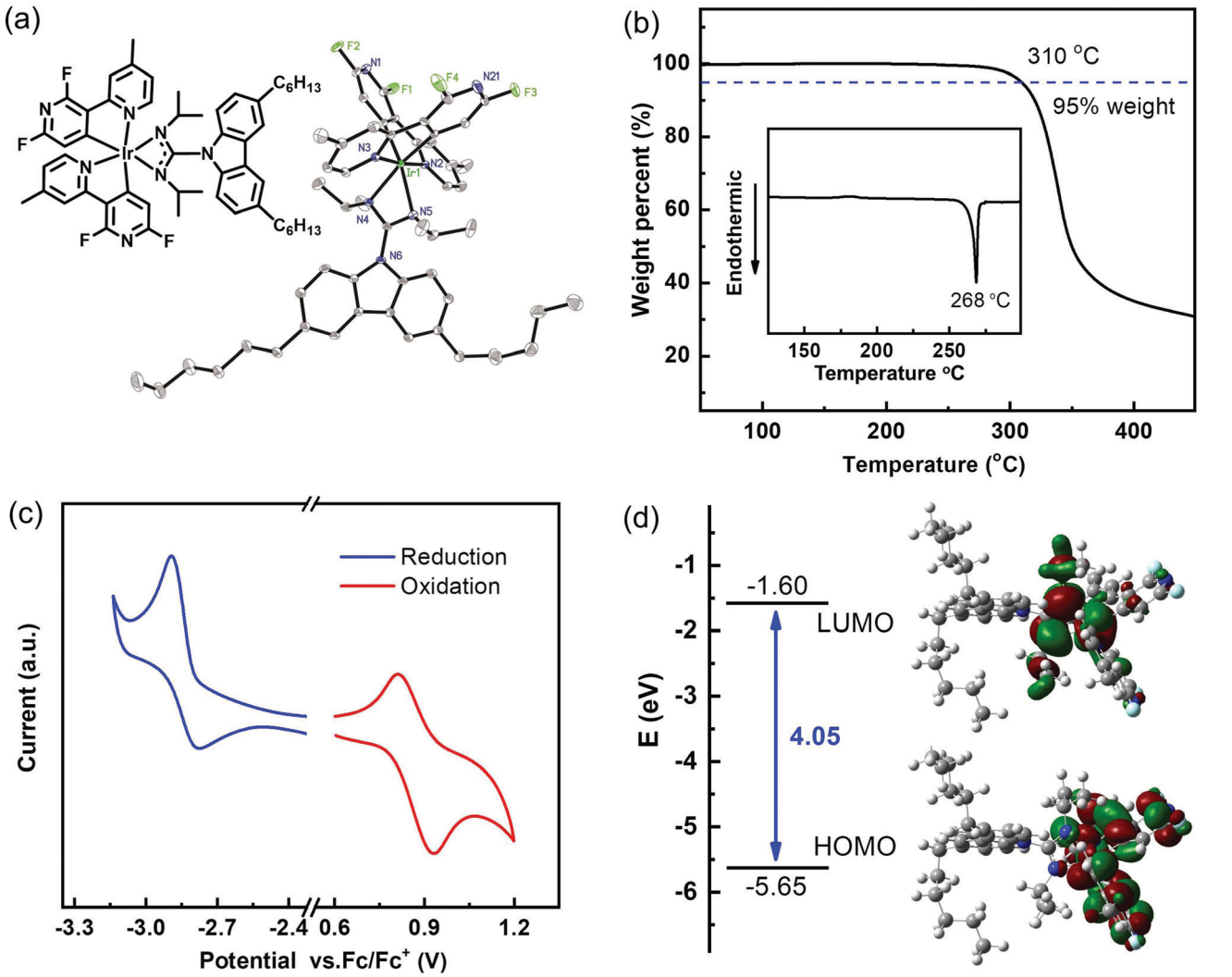

Fig. 1 (a) Molecular structure of **FMPPHC** and its ORTEP plot by X-ray diffraction. (b) Thermal analyses for **FMPPHC**: thermogravimetric analysis (TGA). Inset: Differential scanning calorimetry (DSC). (c) Cyclic voltammetry (CV) of **FMPPHC** in freshly distilled CH_2Cl_2 for oxidation and THF for reduction behavior. (d) Frontier-molecular-orbital distribution and energy levels for **FMPPHC** by DFT calculations.

octahedral geometry around the iridium center. The detailed crystal data and structure refinement are summarized in Table S1 of the ESI.† The thermal property is evaluated by thermogravimetric analysis and differential scanning calorimetry (DSC) (Fig. 1b). The decomposition temperature (Td, corresponding to 5% weight loss) of **FMPPHC** is as high as 310 °C and the glass transition temperature (T_g) of 268 °C is observed. Such good thermal stability can ensure the stable amorphous morphology in the thin film of **FMPPHC**, which is essential for this phosphor to be used as a host or an emitting material. It is an important premise for the fabrication of efficient OLEDs and can effectively enhance the operating lifetime also.

The electrochemical property of **FMPPHC** is carried out by cyclic voltammetry (CV), and the reversible curves of reduction/oxidation behaviors are shown in Fig. 1c, where there is no additional oxidation peak for the electron-rich carbazole fragment, because it has been integrated into the four-membered Ir–N–C–N heterocycle's conjugate system.[23,26] The HOMO (highest occupied molecular orbital) and LUMO (lowest unoccupied molecular orbital) levels are determined as −5.5 eV and −1.9 eV respectively, which are almost consistent with the corresponding values (−5.65 and −1.60 eV) estimated by the density functional theory (DFT) calculations with the Gaussian 09 software at the B3LYP/6-31G(d) level (Fig. 1d and Table 1). On the other hand, a DFT method can investigate deeply the electronic structure of **FMPPHC** and present intuitively the frontier molecular orbital distribution. The HOMO is localized predominantly on the Ir–N–C–N-based central skeleton, while the LUMO is mostly distributed on the two C^N ligands, and they can act as the respective pathways for conducting holes and electrons, ensuring their smooth intermolecular hopping.[27,28] This is a remarkable characteristics of **FMPPHC** possessing good charge carrier transporting properties, and thus this phosphor is expected to be a neat emitter and/or a host for dominating the charge carrier transporting processes in EMLs.

A series of neat and doped films based on FMPPHC and a red dopant phosphor BTPBA[15] are prepared by the spin-coating method from chlorobenzene solvent onto quartz substrates, and their UV/vis absorption and photoluminescence (PL) spectra are shown in Fig. 2a, and the data are summarized in Table 1. Both C^N ligands of **FMPPHC** show strong and sharp absorption peaks of ∼245 nm from the intraligand π–π* transitions, and the relatively low-energy absorption bands of more than 300 nm should be originated from the complexes' spin-allowed singlet metal-to-ligand ^{1}MLCT and ^{1}LLCT transitions. The PL emission peak of the neat **FMPPHC** film is 477 nm, which has a quite narrow full-width at half-maximum (FWHM) value of ∼50 nm. This is a typical sky blue emission with a quite high absolute photoluminescence quantum yield (PLQY) of 0.32 ± 0.05 and short phosphorescence lifetime of 0.8 μs (Fig. S1 in the ESI†), indicating that the singlet/triplet states' efficient spin–orbit coupling and the intersystem crossing of **FMPPHC** induce the emitting excited state to achieve light output efficiently.

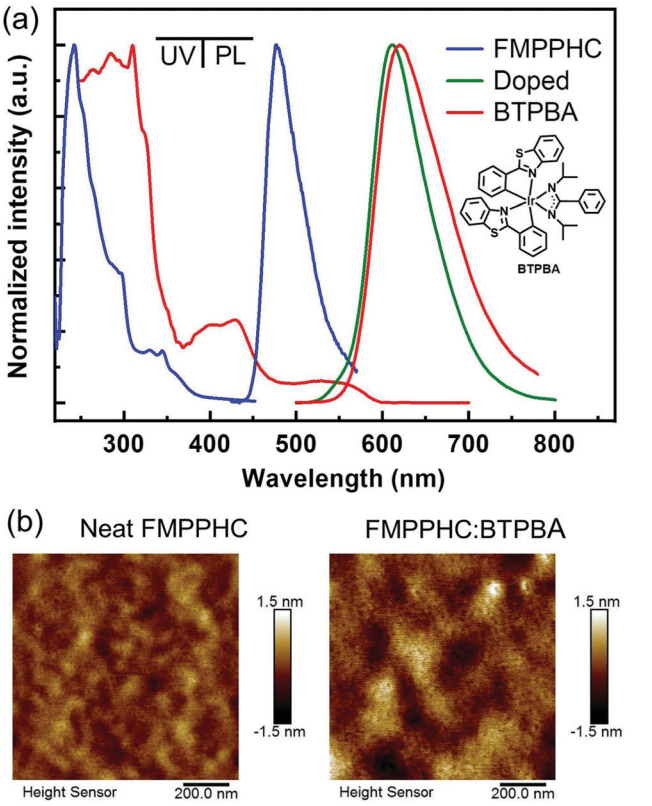

Fig. 2 (a) UV-Vis absorption and PL spectra in neat solid films of **FMPPHC** and BTPBA, and PL spectra in doping solid films of **FMPPHC** (host):BTPBA (dopant) with the doping concentration of 8 wt%. Inset: Molecular structure of BTPBA. (b) AFM topographical images of the solution-processed films of neat **FMPPHC** and **FMPPHC** doped with 15 wt% BTPBA.

Table 1 Photophysical and frontier molecular orbital properties of **FMPPHC**

λ_{abs}[a] [nm]	λ_{em}[a] [nm]	Φ_{PL}[a] [%]	τ_r[a] [μs]	HOMO/LUMO [eV]
245, 300, 331, 346	477	0.32	0.8	−5.50/−1.90;[b] −5.65/−1.60[c]

[a] Measured in neat film at room temperature. [b] Determined from cyclic voltammetry. [c] Estimated by the density functional theory (DFT) calculation.

On the other hand, BTPBA shows a wide MLCT absorption band of 480–590 nm, which has a large overlap with the emission peak (λ_{max}: 477 nm) of **FMPPHC**, and their triplet energy levels are estimated as values of 2.1 and 2.5 eV respectively from the 0–0 band of the phosphorescence spectra,[29] leading to an efficient sensitization process from **FMPPHC** to BTPBA as the complete-energy-transfer PL curve of their doped film (Fig. 2a). Furthermore, **FMPPHC** and BTPBA possess several similar features such as lifetime values and molecular geometry configurations, indicating that this host-dopant combination is suitable for practical applications in constructing efficient emitting systems for PHOLEDs. More than this, the atomic force microscopy (AFM) technique was used to test the film-forming property of **FMPPHC** and its miscibility with

the dopant phosphor BTPBA in spin-coated thin films. Fig. 2b exhibits two AFM height images of the neat film of **FMPPHC** and the doped film with **FMPPHC**:BTPBA (15 wt%). Two images display that both films are the continuous amorphous states in terms of the smooth surface morphology with quite small root mean square (RMS) roughness values of 0.274 nm for the neat film of **FMPPHC** and 0.399 nm for the doping film, which means that **FMPPHC** should form morphologically stable and durable solution-processed films without the obvious particle aggregation or phase separation. All these desirable features are favorable for **FMPPHC** and/or this host-dopant combination to be used in OLED fabrication and operation processes. The foregoing systemic characterizations establish that **FMPPHC** possesses overall optoelectronic features, and thus it has great potential to act as a host and/or emitter for constructing solution-processed OLEDs. Here, three PHOLEDs employing a neat **FMPPHC** film and two **FMPPHC**:BTPBA (15 and 30 wt%) doping films prepared by the spin coating method as EMLs, which are named device NB (neat-blue) and device DR15 and DR30 (doped-red) respectively, are fabricated. These PHOLEDs adopt a unified device configuration of ITO/PEDOT:PSS (40 nm)/EML (40 nm)/TPBi (40 nm)/LiF (1.5 nm)/Al (100 nm), where poly(ethylenedioxythiophene):poly(styrenesulfonate) (PEDOT:PSS) is the hole-injection and -transporting material, 1,3,5-tris (*N*-phenylbenzimidazole-2-yl)benzene (TPBi) is the electron-transporting material, and ITO (indium-tin oxide) and LiF/Al are the anode and cathode, respectively (Fig. 3a). Device NB employing the neat-film emitting system shows an electrophosphorescence emission with λ_{max} = 484 nm with a very narrow FWHM value of 52 nm at the luminance of 1000 cd m^{-2} with quite stable EL spectral curves under different luminance levels (Fig. S2 in the ESI†), which is a sky blue light based on the $CIE_{x,y}$ coordinates of (0.22, 0.37) (Fig. 3b). NB exhibits a low turn-on voltage of 3.2 V, and achieves the maximum EQE/PE values of 16.5%/32.3 lm W^{-1}, which retains the high level of 13.5%/20.8 lm W^{-1} at the practical luminance of 1000 cd m^{-2} (nit), as shown in Fig. 3c and d and summarized in Table 2. To the best of our knowledge, NB is the first report as a nondoped PHOLED based on a neat wet-process film containing only one "pure small-molecule" phosphorescent complex **FMPPHC**, which is neither the polymer phosphorescent complex nor the dendrimer case,[6,11,30] and thus realizes a phosphor-only EML without any fluorescent component. More than this, both the EQE and PE levels of this solution-processed emitting system are not only significantly higher than that of the corresponding cases fabricated by a vacuum deposition process,[31] but also can be comparable with the highest EL efficiencies based

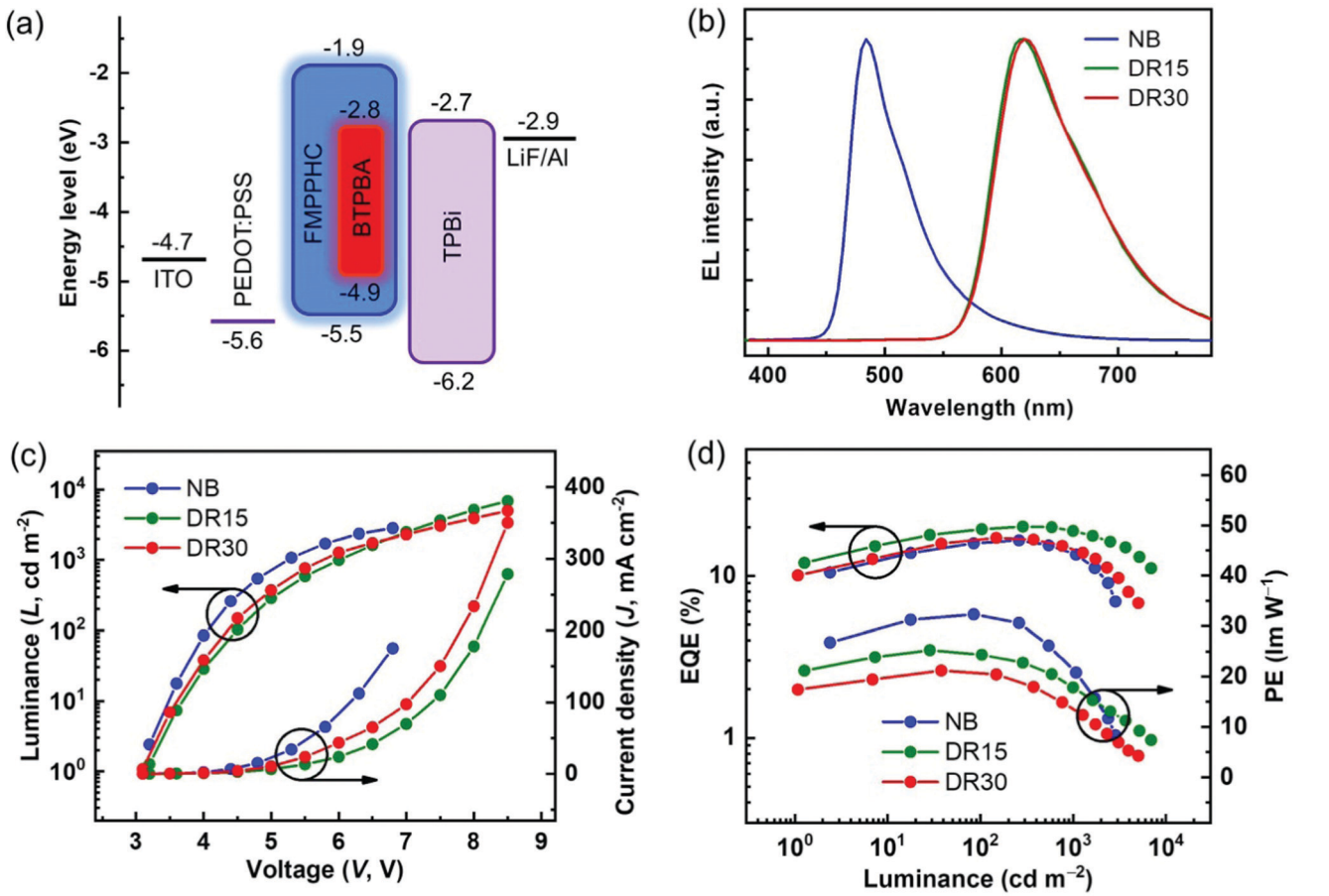

Fig. 3 (a) Proposed energy diagram of the materials used in OLEDs. (b) Normalized EL spectra of devices NB, DR15 and DR30 at the luminance of 1000 cd m^{-2}. Current density–voltage–luminance (*J*–*V*–*L*) curves (c) and power efficiency (PE)–luminance (*L*)–external quantum efficiency (EQE) curves (d) of devices NB, DR15 and DR30.

Table 2 Summary of EL performance for devices NB, DR15 and DR30

Device	$V_{turn\text{-}on}$[a] [V]	PE[b] [lm W^{-1}]	EQE[b] [%]	CIE(x, y)/ λ_{max}[c] [nm]
NB	3.2	32.3, 31.5, 20.8	16.5, 16.2, 13.5	(0.20, 0.37)/484
DR15	3.2	25.3, 24.3, 18.1	20.2, 19.3, 19.0	(0.64, 0.36)/616
DR30	3.1	21.2, 20.8, 15.1	17.1, 16.7, 15.0	(0.64, 0.36)/616

[a] Recorded at 1 cd m^{-2}. [b] In the order of maximum, then values at 100 and 1000 cd m^{-2}. [c] Measured at 1000 cd m^{-2}.

on the self-host phosphorescent dendrimer system through the elaborate molecular structure design as well as the complex synthesis and purification.[6,11] Such desirable EL performance of NB demonstrates that **FMPPHC** inherits the multifunctional features of the Ir–N–C–N-backbone Ir(III) complex family including the remarkable bipolar characteristic and the resulting balanced and sufficient hole/electron flux in the whole EML together with the common high luminous ability and short excited phosphorescent lifetime in their solid state.[24–26] On the other hand, the good film-forming ability/morphological stability of the neat **FMPPHC** film is an equally important determining factor for achieving the exceptional EL performance mentioned above. These results indicate that small-molecule phosphorescent complexes can be basically designed appropriate for solution processes so that the wet-process technology can be comparable with their evaporation process counterparts.

The clear host-molecule characteristics of **FMPPHC** in the non-doped device NB together with the complete host-dopant energy transfer from **FMPPHC** to BTPBA as shown in Fig. 2, indicate that the phosphor–phosphor type (PPT) host-dopant doping emitting system based on **FMPPHC**–BTPBA combination should be efficient. Fig. 3b shows the EL spectra of two doping devices DR15 and DR30 at luminance 1000 cd m^{-2}. They have one-peak (λ_{max} = 616 nm) electrophosphorescence without any host emission, which is the stable saturated red light from BTPBA with the constant CIE$_{x,y}$ coordinates of (0.64, 0.36) within the whole operating voltage range and almost identical to the PL curve of the **FMPPHC**:BTPBA doping film (Fig. 2). The two PPT devices present a similar turn-on voltage of 3.1–3.2 V to NB because all the EL processes of the three devices are dominated by **FMPPHC**, but their J–V and L–V curves o are quite different after turn-on voltage as shown in Fig. 3c, where NB presented more rapidly increasing J and L values than those of both doping cases. According to the energy diagram of the materials used in DR15 and DR30 (Fig. 3a), the red dopant has narrower energy gap (E_g) between the HOMO and LUMO levels than **FMPPHC**, especially for its much deeper LUMO level than that of the host molecule, and thus one of the roles of dopant molecules should be trapping charge carriers from the host sites, leading to the relatively lower J and L levels of DR15 and DR30. On the other hand, the direct holes and/or electrons injected through BTPBA should be promoted with the increasing doping concentrations from 15 to 30 wt%; meanwhile the increasing content of dopant can reduce the molecule space and further enhance the charge transport by hopping, leading to the slightly faster upward trend of the curves of DR30 than those of DR15. Although the doping concentrations of DR15 and DR30 are double the difference, they exhibit comparable EL characteristics in terms of their luminance/current curves and efficiency levels. DR15 and DR30 achieve the high maximum PE and EQE values of 25.3, 21.2 lm W^{-1} and 20.2, 17.1% respectively, which maintain the high levels of 18.1, 15.1 lm W^{-1} and 19.0, 15.0% at a practical luminance of 1000 cd m^{-2}. Such high and stable EL performance based on this solution-processing PPT system can be even competitive with the best red OLEDs reported by evaporation techniques.[15] This stability of EL performance in a certain concentration range (15–30%) demonstrates that this new small-molecule solution processable host phosphor possesses the amazing ability to retain the excellent morphology in its neat film or the corresponding doping films. Nevertheless, it can be seen from Fig. 3d and Table 2 that DR30 showed slightly lower efficiency level together with more significant roll-off than DR15, because the relatively more dopant molecules in the EML of DR30 result in that the increase of the exciton density might gradually exceed the optimal value, which inevitably leads to the probability of triplet–triplet annihilation (TTA) and the resulting decrease of luminance and efficiency levels.

Conclusions

In summary, we design and synthesize a new small molecule phosphorescent Ir(III) complex by incorporating alkyl chains as the solubilizing groups, and meanwhile, the appropriate length of *n*-hexane ensures that **FMPPHC** maintains its inherent excellent optoelectronic properties including high luminous/charge transporting abilities in the solid state. Although without an amazing synthetic process and chemical structure, this phosphors possesses desirable film formation and morphology stability of **FMPPHC**-based films by a wet-process technique, the corresponding emitting systems just employing **FMPPHC** as either a neat blue emitter or a host sensitizing red phosphorescent dopant without any fluorescent component, realize quite high EL performance, which can be even competitive with the best OLEDs reported by evaporation processes. Therefore, this work extends the bipolar phosphor family to wet-process feasible systems, and more importantly, sets an important precedent that small molecule-based phosphorescent complexes not only possess inherent advantages in terms of easy synthesis, purification and emission color tuning, but also are endowed with the amazing ability to form excellent films from solution through simple/feasible molecular structure optimization, like the classical polymer materials.

Conflicts of interest

There are no conflicts to declare.

Note added after first publication

This article replaces the version published on 20th August 2021 which was the Accepted Manuscript of a different article.

Acknowledgements

Ms Y. Feng and Dr J. Xue contributed equally to the work reported in this article. This work was supported by the National Natural Science Foundation of China (51773078 and 21935005).

Notes and references

1 B. W. D'Andrade and S. R. Forrest, *Adv. Mater.*, 2004, **16**, 1585–1595.
2 S.-H. Eom, Y. Zheng, E. Wrzesniewski, J. Lee, N. Chopra, F. So and J. Xue, *Appl. Phys. Lett.*, 2009, **94**, 153303.
3 S. Reineke, F. Lindner, G. Schwartz, N. Seidler, K. Walzer, B. Lussem and K. Leo, *Nature*, 2009, **459**, 234–238.
4 Z. Yang, Z. Mao, Z. Xie, Y. Zhang, S. Liu, J. Zhao, J. Xu, Z. Chi and M. P. Aldred, *Chem. Soc. Rev.*, 2017, **46**, 915–1016.
5 M. Singh, H. M. Haverinen, P. Dhagat and G. E. Jabbour, *Adv. Mater.*, 2010, **22**, 673–685.
6 D. Xia, B. Wang, B. Chen, S. Wang, B. Zhang, J. Ding, L. Wang, X. Jing and F. Wang, *Angew. Chem., Int. Ed.*, 2014, **53**, 1048–1052.
7 H. Xu, R. Chen, Q. Sun, W. Lai, Q. Su, W. Huang and X. Liu, *Chem. Soc. Rev.*, 2014, **43**, 3259–3302.
8 D. Sun, X. Zhou, J. Liu, X. Sun, H. Li, Z. Ren, D. Ma, M. R. Bryce and S. Yan, *ACS Appl. Mater. Interfaces*, 2015, **7**, 27989–27998.
9 Y. Jiang, P. Lv, J.-Q. Pan, Y. Li, H. Lin, X.-W. Zhang, J. Wang, Y.-Y. Liu, Q. Wei, G.-C. Xing, W.-Y. Lai and W. Huang, *Adv. Funct. Mater.*, 2019, **29**, 1806719.
10 X. Liu, Z. Yu, M. Yu, X. Zhang, Y. Xu, P. Lv, S. Chu, C. Liu, W.-Y. Lai and W. Huang, *ACS Appl. Mater. Interfaces*, 2019, **11**, 26174–26184.
11 D. M. Stoltzfus, W. Jiang, A. M. Brewer and P. L. Burn, *J. Mater. Chem. C*, 2018, **6**, 10315–10326.
12 J.-H. Jou, S. Sahoo, D. K. Dubey, R. A. K. Yadav, S. S. Swayamprabha and S. D. Chavhan, *J. Mater. Chem. C*, 2018, **6**, 11492–11518.
13 T. Tsuzuki and S. Tokito, *Adv. Mater.*, 2007, **19**, 276–280.
14 G. Li, D. Zhu, T. Peng, Y. Liu, Y. Wang and M. R. Bryce, *Adv. Funct. Mater.*, 2014, **24**, 7420–7426.
15 Y. Feng, P. Li, X. Zhuang, K. Ye, T. Peng, Y. Liu and Y. Wang, *Chem. Commun.*, 2015, **51**, 12544–12547.
16 P. Arsenyan, A. Petrenko, K. Leitonas, D. Volyniuk, S. J. Imokaitiene, T. Klinavicius, E. Skuodis, J. H. Lee and J. V. Grazulevicius, *Inorg. Chem.*, 2019, **58**, 10174–10183.
17 B. Jiang, X. Ning, S. Gong, N. Jiang, C. Zhong, Z.-H. Lu and C. Yang, *J. Mater. Chem. C*, 2017, **5**, 10220–10224.
18 B. Jiang, C. Zhao, X. Ning, C. Zhong, D. Ma and C. Yang, *Adv. Opt. Mater.*, 2018, **6**, 1800108.
19 S. Kesarkar, W. Mroz, M. Penconi, M. Pasini, S. Destri, M. Cazzaniga, D. Ceresoli, P. R. Mussini, C. Baldoli, U. Giovanella and A. Bossi, *Angew. Chem., Int. Ed.*, 2016, **55**, 2714–2718.
20 X. Yang, H. Guo, B. Liu, J. Zhao, G. Zhou, Z. Wu and W. Y. Wong, *Adv. Sci.*, 2018, **5**, 170106.
21 B. Liu, F. Dang, Z. Feng, Z. Tian, J. Zhao, Y. Wu, X. Yang, G. Zhou, Z. Wu and W.-Y. Wong, *J. Mater. Chem. C*, 2017, **5**, 7871–7883.
22 W. Dang, X. Yang, Z. Feng, Y. Sun, D. Zhong, G. Zhou, Z. Wu and W.-Y. Wong, *J. Mater. Chem. C*, 2018, **6**, 9453–9464.
23 Y. Sun, X. Yang, B. Liu, J. Dang, Y. Li, G. Zhou, Z. Wu and W.-Y. Wong, *J. Mater. Chem. C*, 2019, **7**, 8836–8846.
24 Y. Liu, K. Ye, Y. Fan, W. Song, Y. Wang and Z. Hou, *Chem. Commun.*, 2009, 3699–3701.
25 G. Li, P. Li, X. Zhuang, K. Ye, Y. Liu and Y. Wang, *ACS Appl. Mater. Interfaces*, 2017, **9**, 11749–11758.
26 M. Du, Y. Wang, J. Wang, S. Chen, Z. Wang, S. Wang, F. Bai, Y. Liu and Y. Wang, *J. Mater. Chem. C*, 2019, **7**, 5579–5583.
27 Z. Ge, T. Hayakawa, S. Ando, M. Ueda, T. Akiike, H. Miyamoto, T. Kajita and M.-A. Kakimoto, *Adv. Funct. Mater.*, 2008, **18**, 584–590.
28 Y. Tao, Q. Wang, C. Yang, C. Zhong, K. Zhang, J. Qin and D. Ma, *Adv. Funct. Mater.*, 2010, **20**, 304–311.
29 X. K. Liu, W. Chen, H. Thachoth Chandran, J. Qing, Z. Chen, X. H. Zhang and C. S. Lee, *ACS Appl. Mater. Interfaces*, 2016, **8**, 26135–26142.
30 N. R. Evans, L. S. Devi, C. S. K. Mak, S. E. Watkins, S. I. Pascu, A. Koehler, R. H. Friend, C. K. Williams and A. B. Holmes, *J. Am. Chem. Soc.*, 2006, **128**, 6647–6656.
31 X. Zhuang, X. Liu, S. Chen, H. Zhang, Y. Liu and Y. Wang, *J. Mater. Chem. C*, 2020, **8**, 5355–5360.